Available online www.jocpr.com

Journal of Chemical and Pharmaceutical Research, 2019, 11(12):73-91

Research Article

ISSN: 0975-7384
CODEN(USA): JCPRC5

Theobromine as an Aluminium Corrosion Inhibitor in 1M HCL: Experimental and QSPR Studies

Beda RHB [1], Koffi AA [1], Ehouman D[2], Niamien PM[1*] and Trokourey A[1]

[1]*Laboratoire de Chimie Physique, Université Félix Houphouët Boigny, Abidjan-Cocody, 22 BP 582 Abidjan 22, Côte d'Ivoire*

[2]*Laboratoire de Thermodynamique et Physico-Chimie du Milieu, Université Nangui Abrogoua, 02 BP 801 Abidjan 02, Côte d'Ivoire*

ABSTRACT

The performance of Theobromine (TB) in aluminium corrosion inhibition has been tested. The corrosion inhibition efficiency and the effects of iodide ions were assessed, using mass loss method. The results show that the inhibition efficiency increases with increasing concentration in TB, but decreases with increasing temperature. Adsorption of TB onto the aluminium surface was approximated by the modified Langmuir adsorption isotherm. The thermodynamic adsorption and activation functions were determined. The presence of iodide ions in the environment of the metal led to an increase in inhibition efficiency for temperatures lower than 313 K, but a decrease in corrosion inhibition is remarked for temperatures higher than the mentioned temperature. DFT calculations based on B3LYP/6-31G (d) led to global and local parameters. Some selected sets of these descriptors were correlated with corrosion inhibition efficiency.

Keywords: Aluminium corrosion inhibition; Theobromine; Mass loss; Adsorption isotherm; DFT; Molecular descriptor; QSPR

INTRODUCTION

The key properties of aluminium are its light weight coupled with high strength, good conductivity for electricity and heat, particularly good corrosion resistance including resistance to water and chemicals. All those properties and its universal range of uses mean it can be found everywhere. Aluminium is a very reactive metal with high affinity for oxygen; the metal is highly resistant due to the inert and protective oxide film formed on its surface. Therefore, in some aggressive environments the metal is dissolved (corroded).

A variety of protection methods are used to enhance aluminium and its alloys corrosion resistance. Amongst the most common methods is the use of organic molecules to combat the dissolution of metals. These molecules [1-3] contain nitrogen, oxygen, sulphur and phosphorus with lone pairs as well as π-electrons which can interact with the metal, favouring the adsorption process. So, according to the literature, many molecules have been tested: azoles [4,5], amines [6,7], drugs [8-10], etc.

The literature [11,12] mentioned that to enhance the performance of organic molecules on metal corrosion inhibition, the use of halide ions as Cl^-, F^- and I^- is an effective means, since it improves the inhibiting force of organic inhibitors.

Several DFT calculations [13-15] show a link between inhibition efficiency and structure/electronic properties of organic molecules, used as corrosion inhibitors. So, molecular descriptors as EHOMO (Energy of the Highest Occupied Molecular Orbital), ELUMO (Energy of the Lowest Unoccupied Molecular Orbital), ΔE (the energy gap), the global electronegativity (χ), the global hardness (η) and softness (σ) and local descriptors as Fukui functions(f_k^+ or f_k^-) and dual descriptors (Δf_k^+ or Δf_k^-) have been used to describe the mechanisms of corrosion inhibition based on the interactions between the metal and the organic molecules.

QSPR (Quantitative Structure-Property Relationship) is a modelling approach applied in corrosion inhibition of metal. This approach [16] provides mathematical relations which indicate correlations between some sets of descriptors and the corrosion performance of a molecule.

The objective of this paper is firstly to study the inhibition properties of Theobromine alone and in association with some iodide ions. Secondly, this work aims to determine the possible correlations between some sets of descriptors and the inhibition efficiency of the studied molecule.

MATERIALS AND METHODS

Aluminium Specimens

The aluminium samples of purity 99.5% were in the form of rod measuring 10 mm in length and 2 mm in diameter.

The Studied Molecule

The structure of Theobromine (formula: $C_7H_8N_4O_2$) is given in Figure 1.

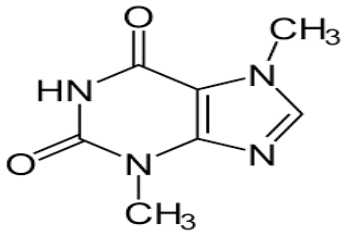

Figure 1. Chemical structure of Theobromine

Solutions

Analytical grade, 37% HCl from Merck was used to prepare the blank of 1 M. Theobromine (purity ≥ 98%) from Aldrich Chemicals was used and solutions of concentrations range from 0.0001 M to 0.005 M were prepared.

Sodium iodide (formula: NaI, purity ≥ 99.5%) a water soluble iodide salt from Sigma Aldrich was used to prepare solutions of concentration 0.01M.

Mass Loss Studies

Aluminium of 99.5% purity was used for mass loss studies. The samples were polished with fine emery papers, cleaned with acetone, washed with double distilled water and dried in a desiccator. The samples were then weighed and immersed in 50 mL of an aerated 1.0 M HCl solution without or with the desire concentration of Theobromine. After one hour exposure, the samples were retrieved from the solution, washed abundantly with water, dried and weighed using an analytical balance (precision: ± 0.1 mg). The experiments were carried at temperatures range from 298-323K. The corrosion rate and the inhibition efficiency were respectively calculated using the following equations:

$W=\Delta m/St$ (1)

$$IE(\%) = \frac{W_0 - W}{W_0} \times 100 \quad (2)$$

Where Δm is mass loss, S is the sample total surface, t is the immersion time, and W_0 and W are respectively the corrosion rate without and with theobromine.

Quantum Chemical Calculations

The optimization of the molecule of Theobromine was realised using Density Functional Theory (DFT) at the level B3LYP/6-31 G (d) with the Gaussian 09 Program [17]. The exchange correlation functional [18,19] is given by the equation below:

$E_{XC}=a_0 E_X (HF)+a_1 E_X (LSD)+a_2 E_X (GGA)+a_3 E_C$ (3)

Where E_X (HF) represents the Hartree exchange energy, E_X (LSD) is the Dirac exchange energy and E_X (GGA) is the gradient corrections to exchange energy B88 form and Lee-Yang- Parr (LYP) functional.

The basis set 6-31G (d) is a Double Zeta (DZ) basis set where 6 denotes the number of Gaussians that represent each core basis function, and 3 and 1 represent the number of Gaussians for the split valence basis functions. This basis set adds d functions to second row elements (C, O, N, etc).

RESULTS AND DISCUSSION

Mass Loss Results

Effect of concentration: The inhibition efficiency of Theobromine acquired from mass loss method in 1 M HCl solution for different concentrations of the inhibitor is given in Figure 2.

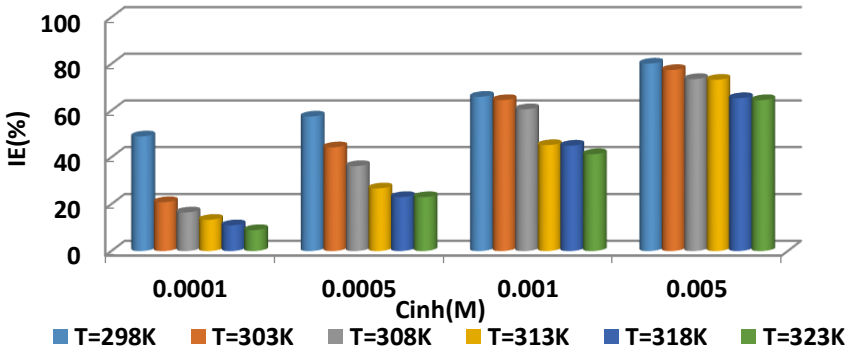

Figure 2. Inhibition efficiency of Theobromine for different concentrations and temperatures

It is clear from Figure 2 that the inhibition efficiency of Theobromine increases when its concentration increases for all the studied temperatures.

These results indicate that TB acts as an effective inhibitor for aluminium corrosion in 1 M HCl. This behaviour can be explained by the adsorption of the molecules onto the aluminium surface, isolating the metal surface from the corrosive environment. Similar results [8,20] are reported in the literature.

Effect of the temperature: The evolution of the inhibition efficiency of TB *versus* the temperature is given by Figure 3. In this Figure, one can observe that the corrosion inhibition decreases with increasing temperature for all the studied concentrations.

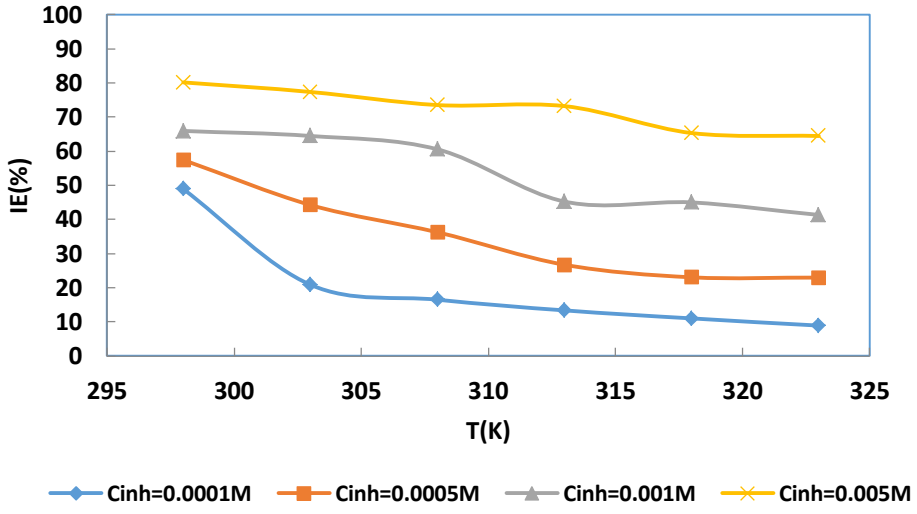

Figure 3. Inhibition efficiency *versus* temperature for different concentration in TB

This evolution of the inhibition efficiency with temperature can be explained [21] by the weakening of the adsorption driving strength and/or by desorption of the inhibitor from the aluminium surface when the temperature increases. So, for C_{inh}=0.0001 M, the inhibition efficiency IE (%)=48.92 for T=298K and its value is IE (%)=8.92 for T=323K.

Adsorption Consideration

The adsorption of organic molecules onto the surface of a metal [22] is considered as a substitutional adsorption process between the organic molecule in aqueous phase $Org_{(sol)}$ and the water molecules $H_2O_{(ads)}$ adsorbed onto the metal surface:

$$Org_{(sol)} + xH_2O_{(ads)} \rightleftarrows Org_{(ads)} + xH_2O_{(sol)} \qquad (4)$$

Where x is the number of water molecules replaced by one organic molecule.

To determine the adsorption mode, various isotherms (Langmuir, El-Awady, Temkin, Flory Huggins and Freundlich) were considered. Though the Langmuir isotherm (plots in Figure 4) was found to be the best, the deviation from the basic assumptions (slope different from unity) of the model shows that it cannot applied rigorously.

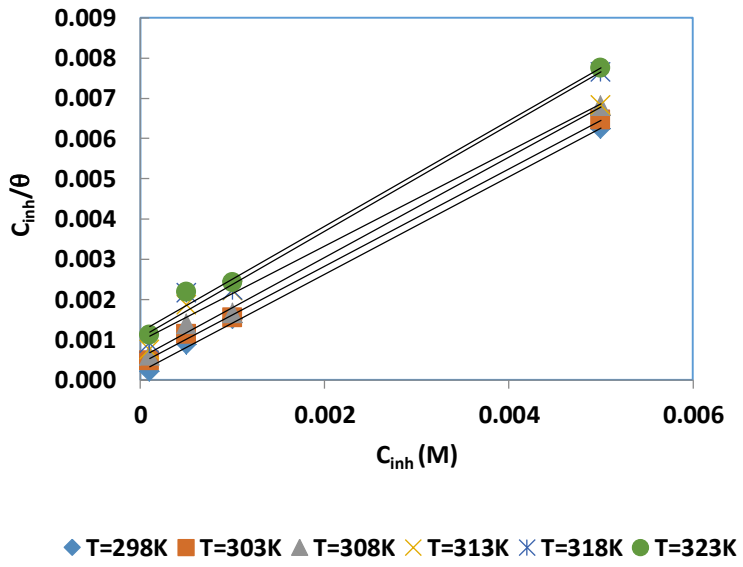

Figure 4. Langmuir isotherm adsorption plots for TB onto aluminium in 1 M HCl

The problem is solved by Villamil adsorption isotherm [23], a modified Langmuir adsorption isotherm which is described by the equation below

$$\frac{C_{inh}}{\theta} = \frac{n}{K_{ads}} + nC_{inh} \qquad (5)$$

Where $n\theta$ is the effective covered surface fraction of the metal. Table 1 gives the Villamil adsorption parameters.

Table 1. Modified Langmuir adsorption isotherm parameters

T(K)	Equation	R^2	Kads (M^{-1})	ΔG°_{ads}	ΔH°_{ads}	ΔS°_{ads}
298	C_{inh}/θ=1.210Cinh+0.0002	0.999	6050.0	-31.51	-78.41	-157.7
303	C_{inh}/θ=1.210Cinh+0.0004	0.999	3025.0	-30.29		
308	C_{inh}/θ=1.210Cinh+0.0005	0.997	2420.0	-30.22		
313	C_{inh}/θ=1.210Cinh+0.0010	0.990	1210.0	-28.91		
318	C_{inh}/θ=1.210Cinh+0.0011	0.989	1100.0	-28.26		
323	C_{inh}/θ=1.210Cinh+0.0012	0.994	1008.3	-27.47		

The calculated equilibrium constant K_{ads} in Table 1 was obtained by using the following equation:

$$\Delta G^0_{ads} = -RTln(55{,}5 \times K_{ads}) \qquad (6)$$

Where R is the universal constant, T is the temperature and 55.5 is the water concentration solution in mol.L^{-1}.

The variation of free adsorption enthalpy ΔG^0_{ads} is negative, indicating a spontaneous adsorption process. All the calculated values are higher than -40 kJ.mol^{-1}, but lower than -20kJ.mol^{-1}, showing [24] that both physical and chemical adsorption processes are involved.

The variation of the adsorption enthalpy ΔH^0_{ads} and that of the adsorption entropy ΔS^0_{ads} in Table 1 were determined by using the plot of ΔG^0_{ads} *versus* temperature ($\Delta G^0_{ads} = \Delta H^0_{ads} - T\Delta S^0_{ads}$).The obtained values ($\Delta H^0_{ads}$ = -78.41 kJ mol^{-1}) and ($\Delta S^0_{ads} = -157.7$ J$mol^{-1}K^{-1}$) from Figure 5, indicate respectively an exothermic adsorption process and a diminution of disorder probably due to the weakening of the adsorption driving force or the desorption of the adsorbed molecules of the inhibitor with increasing temperature.

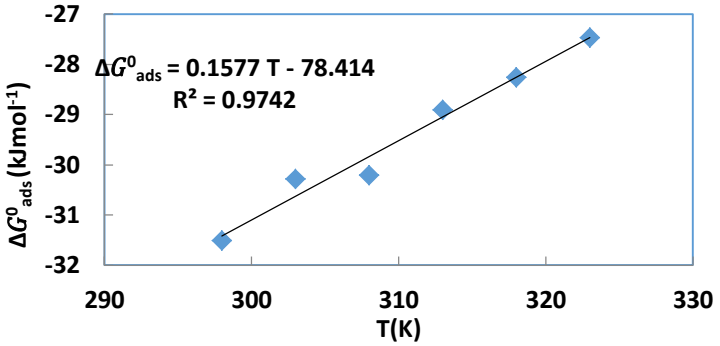

Figure 5. Variation of free enthapy *versus* temperature

In order to go insight the adsorption type we used Adejo-Ekwenchi and Dubinin Radushkevich isotherms.

Adejo-Ekwenchi isotherm

This isotherm [25] is described by the following equation:

$$log\left(\frac{1}{1-\theta}\right) = logK_{AE} + blogC_{inh} \qquad (7)$$

Where K_{AE} and b are the isotherm parameters and C_{inh} is the adsorbate concentration. Figure 6 gives the plots related to the isotherm.

The parameters related to the adsorption are listed in Table 2.

Table 2. Adejo-Ekwenchi adsorption isotherm parameters

T(K)	Equation	R^2	b	K_{AE}
298	log (1/1-θ)=0.2437 log C_{inh}+ 1.2258	0.933	0.2437	16.82
303	log (1/1-θ=0.3302 log C_{inh} + 1.4029	0.968	0.3302	25.29
308	log (1/1-θ)=0.3055 log C_{inh} + 1.2760	0.947	0.3055	18.88
313	log (1/1-θ)=0.3037 log C_{inh} + 1.2146	0.903	0.3037	16.39
318	log (1/1-θ)=0.2485log C_{inh} + 1.0029	0.926	0.2485	10.07
323	log (1/1-θ)=0.2452 log C_{inh} + 0.9810	0.935	0.2452	09.57

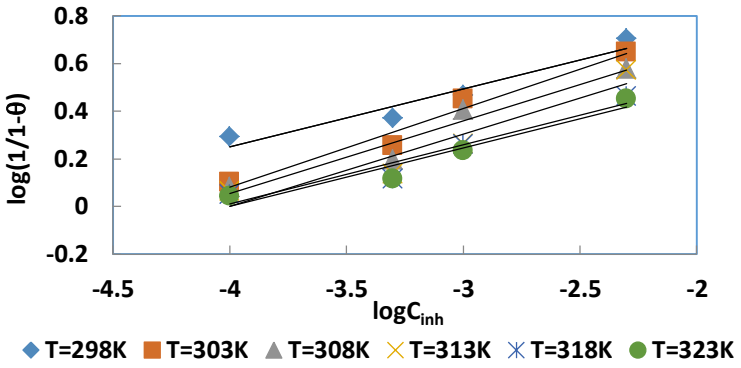

Figure 6: Adejo-Ekwenchi plots for TB adsorption onto aluminium in 1.0M HCl

Analysing Table 2, one can see that the parameters b and K_{AE} increase when going from T=298K to T=303K, showing [25] a chemisorption process. For T=303K to 323K, we note a decrease in the values of both b and K_{AE} parameters showing [25] a physisorption process. These observations confirm the existence of both physisorption and chemisorption.

Dubinin Radushkevich Isotherm

This adsorption [26] is used to distinguish between physical and chemical adsorption. The equation related to the theory is:

$$ln = ln\theta_{max} - a\delta^2 \quad (8)$$

Where θ_{max} is the maximum surface coverage and δ is the Polanyi potential given by:

$$\delta = RTln(1 + \frac{1}{C_{inh}}) \quad (9)$$

The constant δ gives the mean adsorption energy, E_m which is the transfer energy of 1 mole of adsorbate from infinity (bulk solution) to the surface of the adsorbent:

$$E_m = \frac{1}{\sqrt{2a}} \quad (10)$$

Figure 7 gives the plots of this isotherm.

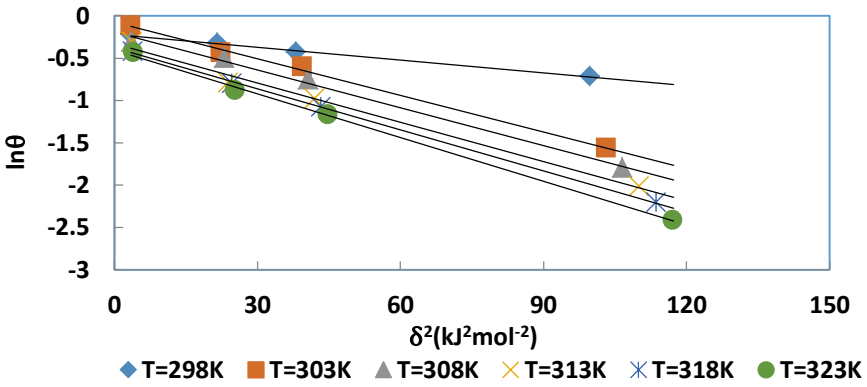

Figure 7. Dubinin adsorption plots for TB onto aluminium

Table 3 gives the parameters of the Dubinin Radushkevich isotherm.

Table 3. Dubinin Radushkevich isotherm equations and parameters

T(K)	Equation	R^2	θ_{max}	a (kJ^{-2} mol^2)	E_m ($kJmol^{-1}$)
298	lnθ=-0.0051δ^2-0.2188	0.994	0.80	0.0051	9.90
303	lnθ=-0.0135δ^2_0.0946	0.999	0.92	0.0146	6.08
308	lnθ=-0.0149δ^2_0.1945	0.994	0.82	0.0149	5.79
313	lnθ=-0.0155δ^2_0.3299	0.990	0.72	0.0155	5.68
318	lnθ=-0.0161δ^2_0.3800	0.999	0.68	0.0161	5.57
323	lnθ=-0.0172δ^2_0.4037	0.999	0.67	0.0172	5.39

These results confirm the weakening of the adsorption driving force (θ_{max} increases for temperatures range from T=298K to T=303K, and the decreases for all the other studied temperatures) and the existence of both chemical adsorption ($E_m \geq 8$ kJmol^{-1}) and physical adsorption ($E_m < 8$ kJmol^{-1}).

Activation Parameters

To determine the kinetic and thermodynamic dissolution parameters of the aluminium in the aggressive solution of 1M HCl, we used Arrhenius and transition state equations:

$$logW = logA - \frac{E_A}{2.303RT} \quad (11)$$

$$log\left(\frac{W}{T}\right) = log\left(\frac{R}{\aleph h}\right) + \frac{\Delta S_a^*}{2.303R} - \frac{\Delta H_a^*}{2.303RT} \quad (12)$$

Where E_A is the apparent activation energy, R is the universal gas constant, A is the frequency factor, h is the Planck's constant, $\aleph$ is the Avogadro number, ΔS_a^* is the change in activation entropy and ΔH_a^* is the change in activation enthalpy.

Activation Energy

Figures 8 and 9 gives respectively the plots of $logW$ and log (W/T) *versus* $1/T$.

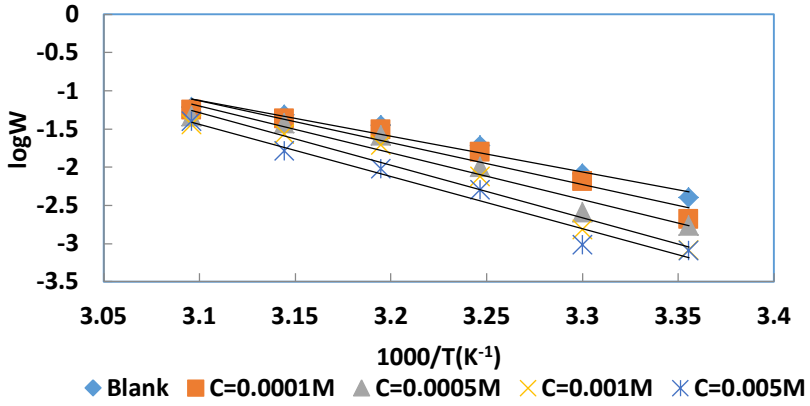

Figure 8. Arrhenius plots for the Blank and different concentrations of TB

All the plots are straight lines from which we deduced the parameters related to the activation process. Table 4 contains all the activation parameters.

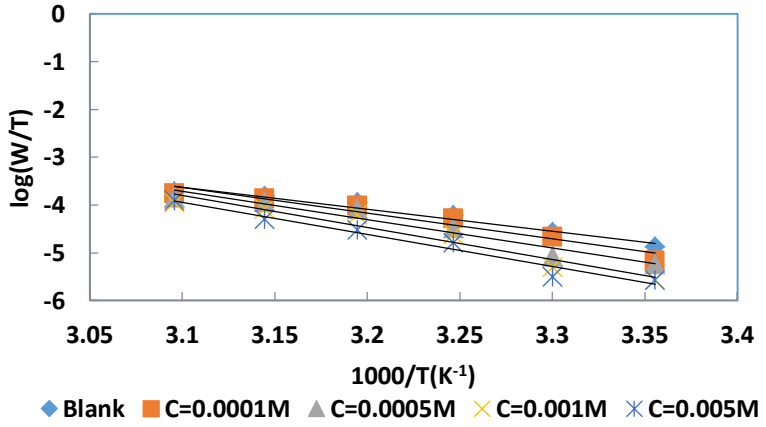

Figure 9. Transition states plots for the blank and different concentrations in TB

Table 4. Dissolution parameters of aluminium in Blank and in various solutions containing TB

Concentration (M)	E_a $(kJmol^{-1})$	ΔH_a^* $(kJmol^{-1})$	ΔS_a^* $(Jmol^{-1}K^{-1})$
Blank	89.77	87.19	11.90
0.0001	105.00	102.42	50.39
0.0005	109.48	114.28	85.74
0.0010	123.66	128.38	127.78

0.0050	131.10	128.52	125.48

The apparent activation energy was calculated, using the plot ($-\frac{E_A}{2.303R}$) of the Arrhenius plot. ΔH_a^* and ΔS_a^* derived respectively from [$log\left(\frac{R}{\aleph h}\right)+\frac{\Delta S_a^*}{2.303R}$] (intercept) and ($-\frac{\Delta H_a^*}{2.303R}$) (slope) of the transition states plots.

Observing the apparent energy (E_A) values, one can noticed that they are higher in presence of TB than that obtained for the blank, what indicates [27,28] that physical adsorption is predominant.

All the values of the change in dissolution enthalpy (ΔH_a^*) are positive, indicating [29] that the dissolution of aluminium is an endothermic process. The change in entropy (ΔS_a^*) has a positive sign for the blank and for all the concentration in TB, suggesting [30] that the activated complex in the rate determining step is a dissociation rather than an association. Moreover, the positive sign of change in activation entropy, indicate an increase in disorder, probably [30] due to the desorption of the adsorbed species.

Effects of the Presence of Iodide Anions

The effect of iodide anion was studied. So, the samples were immersed in different solutions (blank, blank containing iodide anions, blank containing TB and iodide anions) during one hour. The different corrosion rates are given in Figure 10.

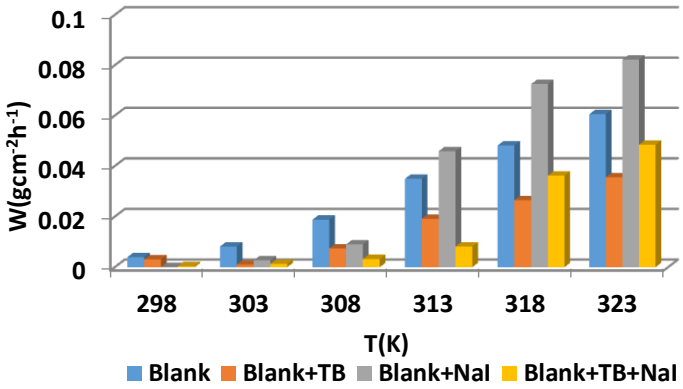

Figure 10. Aluminium corrosion rate for different solutions

From Figure 10, one can see that the presence of iodide anions reduce the corrosion rate for temperature range from T=298 K to T=313 K, probably [31] due to the adsorption of TB onto adsorbed iodide anions (synergistic effect) which form intermediate bridges between positively charged surface metal and the positive end of the organic molecule. In the case of temperatures higher than T=313K, the corrosion is enhanced, what could be explained by the weakening of the adsorption driving force.

Quantum Chemical Studies

Global reactivity parameters: DFT calculations in gas phase at B3LYP/6-31 G (d) led to the molecular quantum chemical and reactivity parameters. Figure 11 shows the optimized studied molecule and all the calculated parameters are collected in Table 5.

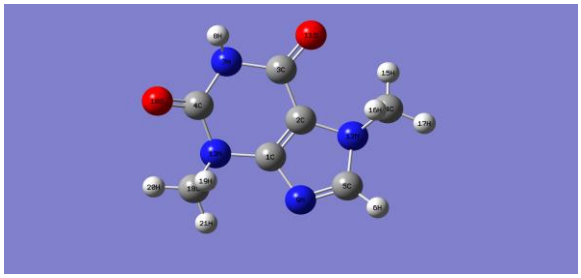

Figure 11. Optimized structure of Theobromine by B3LYP/6-31G (d)

Table 5. Molecular and reactivity parameters of Theobromine by B3LYP/6-31G (d)

Parameters	Value
E_{HOMO} (eV)	-6,042
E_{LUMO} (eV)	-0,897
ΔE(eV)	5,145
$\mu(D)$	4,339
I (eV)	6,042
A (eV)	0,897
χ (eV)	3,469
η (eV)	2,572
σ (eV^{-1})	0,389
ΔN	0,158
ω	2,339
Energie totale (Ha)	-641,045

The energy molecular parameters give very important information on the interactions between the molecule and the metal. So, E_{HOMO}, the highest occupied molecular orbital energy [32,33] is often associated to electron donation; high value of this parameter indicates a good tendency to donate electron to an empty orbital with low energy of the other part of the interface (metal). In our case the value of (-6.042 eV) can be considered [34,35] as a high value when compared to values in the literature.

E_{LUMO}, the lowest unoccupied molecular orbital [36] gives information on the ability of the molecule to accept electron. According to the literature, a molecule with a low value of E_{LUMO} [37] can easily accept electron from an occupied orbital of a metal. So, in general [37], a good corrosion inhibitor should have a high E_{HOMO} value, a low E_{LUMO} value, and a low energy gap ($\Delta E = E_{LUMO} - E_{HOMO}$). In this study the values (E_{LUMO}=-0.897 eV and ΔE=5.145 eV) shows that TB has good inhibition properties. The HOMO-LUMO diagrams are presenting by Figure 12.

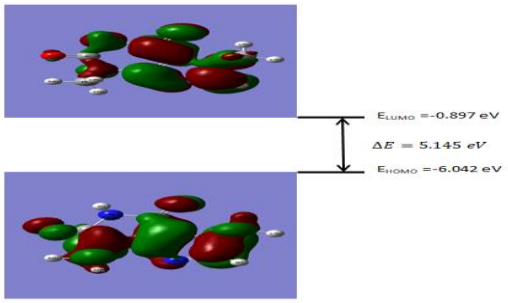

Figure 12. LUMO-HOMO plots (ground state) and energy diagram of Theobromine

The dipole moment(μ) is an index used for the prediction of the corrosion process. It measures the polarity in a bond and is related to electrons distribution in a molecule. Unfortunately, the literature [38] is inconsistent on the use of this parameter for corrosion inhibition.

According to Koopman's theorem [39,40], the negative value of E_{HOMO} defines the ionization potential (***I***) expressed as follows:

$$I = -E_{HOMO} \quad (13)$$

Similarly, the negative value of E_{LUMO} corresponds to the electron affinity (***A***) which is another global reactivity parameter [41] is given by:

$$A = -E_{LUMO} \quad (14)$$

The electronegativity is related to the chemical potential (μ_P) by the following equation:

$$\chi = -\mu_P = \left(\frac{\partial E}{\partial N}\right)_{v(r)} \quad (15)$$

Where N is the number of electrons, $v(r)$ is the external potential of the system and E is the total energy. The electronegativity [42] which measures the power of an atom or a group of atoms to attract electrons towards itself can be written as:

$$\chi = \frac{I+A}{2} \quad (16)$$

The global hardness (η) and the global softness (σ) are two other reactivity parameters. The global hardness [43] which measures the resistance of an atom to charge transfer can be assessed by using the following equation:

$$\eta = \frac{I-A}{2} \quad (17)$$

The global softness [44], the reciprocal of the global hardness which measures the capacity of an atom or a group of atoms to receive electrons is given as follows:

$$\sigma = \frac{1}{\eta} = \frac{2}{I-A} \quad (18)$$

When a molecule and a metal [45] are in contact, electrons are transferred from the system with low electronegativity value to that of high electronegativity value. The fraction of electrons transferred is given by:

$$\Delta N = \frac{\chi_M - \chi_i}{2(\eta_M + \eta_i)} \quad (19)$$

The indices M and i denote metal and inhibitor.

The use of χ_M [46] is conceptually wrong because electron-electron interaction must be taken into account; so the appropriate quantity is the work function ϕ_M. Therefore, the formula is:

$$\Delta N = \frac{\phi_M - \chi_i}{2(\eta_M + \eta_i)} \quad (20)$$

In this work, the theoretical values of ϕ_{Al}= 4.28 eV [47] and hardness η_{Al}= 0 [48] have been used for the aluminium.

The global electrophilicity index (ω) [49,50], another reactivity parameter which indicate the ability of a molecule to accept electrons is given as follows:

$$\omega = \frac{\mu_P^2}{2\eta} \quad (21)$$

A perusal of the literature shows that the calculated values of electronegativity ($\chi = 3.469\ eV$), hardness and softness ($\eta = 2{,}572\ eV$ and $\sigma = 0.389\ (eV^{)-1}$), fraction of electron transfer ($\Delta N = 0.158$) are indicative of the good inhibiting performance of Theobromine.

Local Reactivity Parameters

The inhibition of metal corrosion is governed by donation and acceptance of electrons, what involve the molecular nucleophilic or electrophilic characters. This information can be assessed by the local reactivity parameters as Fukui functions or the Dual descriptor.

The Fukui [51,52] functions expressed using the limit difference approximation is given as follows:

$$f_k^+(r) = \left(\frac{\partial \mu_P}{\partial v(r)}\right)_N^+ = q_k(N+1) - q_k(N) \qquad (22)$$

$$f_k^-(r) = \left(\frac{\partial \mu_P}{\partial v(r)}\right)_N^- = q_k(N) - q_k(N-1) \qquad (23)$$

Where f_k^+ and f_k^- are respectively nucleophilic and electrophilic Fukui functions,$q_k(N+1)$, $q_k(N)$ and $q_k(N-1)$ are the electronic population of atom k in cationic, neutral and anionic forms.

The dual descriptor [53,54] which allows the determination of individual sites within the molecule with particular behaviour is given by the following equation:

$$\Delta f_k(r) = \left(\frac{\partial f_k(r)}{\partial N}\right)_{v(r)} \qquad (24)$$

The condensed form of the dual descriptor is given by the equation:

$$\Delta f_k(r) = f_k^+(r) - f_k^-(r) \qquad (25)$$

All the local parameters are collected in Table 6.

Table 6: Mulliken atomic charges, Fukui functions and dual descriptor by B3LYP/6-31 G (d)

Atom	$q_k(N-1)$	$q_k(N)$	$q_k(N+1)$	f_k^-	f_k^+	Δf_k
1 C	0.542911	0.475393	0.425998	-0.067518	-0.049395	0.018123
2 C	0.305343	0.218518	0.191857	-0.086825	-0.026661	**0.060164**
3 C	0.694809	0.626038	0.497913	-0.068771	-0.128125	-0.059354
4 C	0.813881	0.773343	0.740799	-0.040538	-0.032544	0.007994
5 C	0.283092	0.220853	0.060127	-0.062239	-0.160726	**-0.098487**
6 C	0.251547	0.170965	0.062401	-0.080582	-0.108564	-0.027982
7 N	-0.722451	-0.723416	-0.707495	-0.000965	0.015921	0.016886
8 H	0.407198	0.355862	0.307444	-0.051336	-0.048418	0.002918
9 N	-0.443978	-0.510076	-0.548614	-0.066098	-0.038538	0.027560
10 O	-0.393600	-0.516417	-0.595535	-0.122817	-0.079118	0.043699
11 O	-0.417549	-0.525936	-0.638330	-0.108387	-0.112394	-0.004007
12 N	-0.497026	-0.480928	-0.486200	0.016098	-0.005272	-0.021370
13 N	-0.549797	-0.577557	-0.555692	-0.027760	0.021865	0.049625
14 C	-0.369711	-0.317091	-0.294186	**0.052620**	0.022905	-0.029715
15 H	0.256440	0.200180	0.178762	-0.056260	-0.021418	0.034842
16 H	0.232835	0.200118	0.104643	-0.032717	-0.095475	-0.062758
17 H	0.232829	0.168209	0.106840	-0.064620	-0.061369	0.003251
18 C	-0.351577	-0.322755	-0.299172	0.028822	**0.023583**	-0.005239
19 H	0.241466	0.182819	0.141723	-0.058647	-0.041096	0.017551

20 H	0.241466	0.182810	0.167558	-0.058656	-0.015252	0.043404
21 H	0.241872	0.199069	0.139159	-0.042803	-0.059910	-0.017107

Analysing Table 6, one can see that according to the Fukui functions C (14) with the highest value of f_k^- is the electrophile attack centre whereas C (18) with maximum value of f_k^+ is the nucleophilic attack centre.

Regarding the dual descriptor, one can see that Δf_k has a positive sign for C (2) and a negative sign for C (5). Therefore C (2) is the nucleophile attack centre and C (5) is the electrophilic attack centre.

According to the literature [55] state that although Fukui function has the capability to reveal nucleophilic and electrophilic regions in a molecule, the dual descriptor is the only descriptor which is able to unambiguously expose truly the nucleophilic and electrophilic regions. So, one can retain C (2) and C (5) as respectively the nucleophilic and the electrophile attacks centres.

QSPR Approach

The inhibition efficiency of organic compounds [56-58] is essentially dependent to their properties/descriptors parameters. QSPR, Quantitative Structure Property Relationship is a mathematical approach which attempts to relate the structure derived features of a compound to its biological or physicochemical activity. The chemical structure is represented at molecular level by some sets of descriptors that can mathematically be connected to experimental properties.

In this work, attempts are made to correlate some sets of composite indexes (quantum chemical and reactivity parameters) with the experimental corrosion inhibition efficiency of Theobromine. We used the non-linear model of Lukovits et al. [59] which is given as follows:

$$IE_{calc}(\%) = \frac{(Ax_j+B)C_i}{1+(Ax_j+B)C_i} \times 100 \qquad (26)$$

Where A and B are real constants determined by solving the system of simultaneous equations obtained from different values of the inhibitor concentration C_i. In this equation a quantum chemical parameter is represented by x_j.

In our work taking the number of concentrations into account, we have tested many sets of three parameters. So, the equation becomes:

$$IE(\%) = \frac{(Ax_1+Bx_2+Dx_3+E)C_i}{1+(Ax_1+Bx_2+Dx_3+E)C_i} \times 100 \qquad (27)$$

The concentrations range from 100 µM to 5000 µM. All the calculations have been performed using the EXCEL software and only the sets of parameters that led to a correlation coefficient($R^2 > 0.8$) are presented. The calculated constants (A, B, D and E) of the different sets of parameters are collected in Table 7.

Table 7. Calculated constants of the different sets of parameters

Set of parameters	A	B	D	E
(E_{LUMO}, ΔE, µ)	-2155.36981	-48.374282	-1065.21409	2937.48866
(E_{LUMO}, ΔE, ω)	-4521.78335	-326.17065	-798.24162	-510.79777
(E_{LUMO}, E_{HOMO}, µ)	-1743.29097	0.00108	-1111.70251	3259.95732
(E_{LUMO}, ΔE ,η)	-1347.45136	-157.58537	1173.30871	-3415.63289
(E_{HOMO}, ΔE ,µ)	-440.21334	319.48565	-1959.15943	4197.27566
(E_{HOMO}, ΔE ,η)	-209.34866	-26.23130	1641.57548	-5352.05314

(χ, μ η)	-795.36388	-489.61694	2170.92735	-700.05424
(χ, μ ,ω)	215.36118	-286.75700	-0.002420	497.165870

The calculated inhibition efficiencies *versus* experimental efficiencies plots are shown in Figures 13A-13H. In order to determine the best set of parameters, we used three statistical parameters:

The sum of square errors:

$$SSE = \sum_{i=1}^{N}\left[IE_{exp} - IE_{calc}\right]^2 \qquad (28)$$

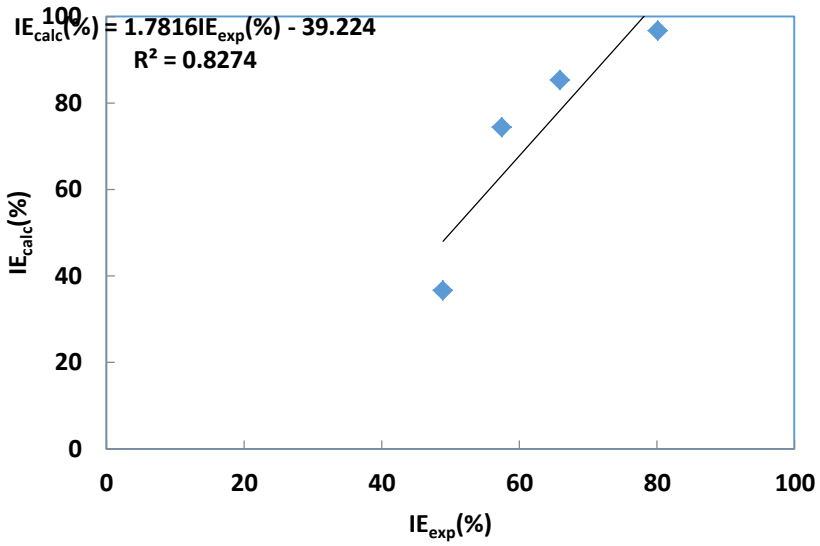

Figure 13A. Correlation between calculated and experimental inhibition efficiencies for (E_{LUMO}, ΔE, μ)

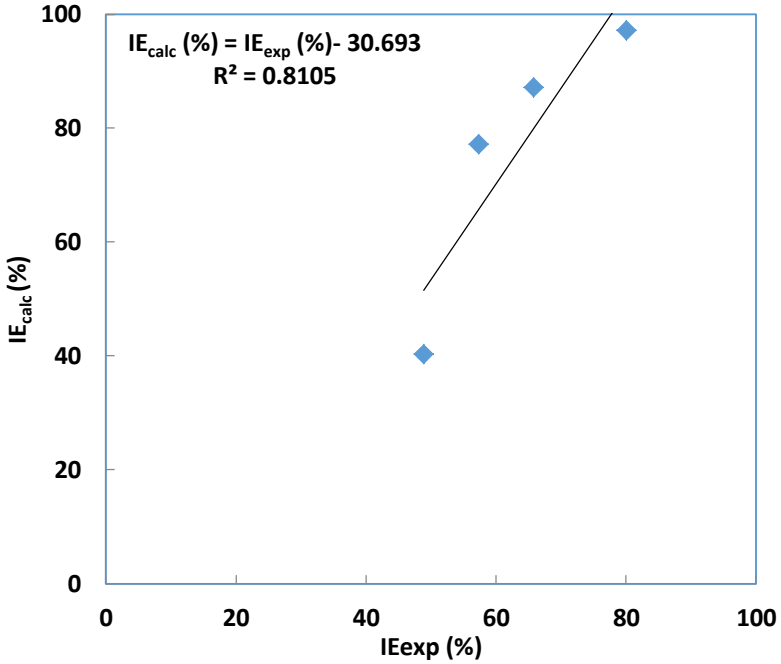

Figure 13B. Correlation between calculated and experimental inhibition efficiencies for (E_{LUMO}, ΔE, ω)

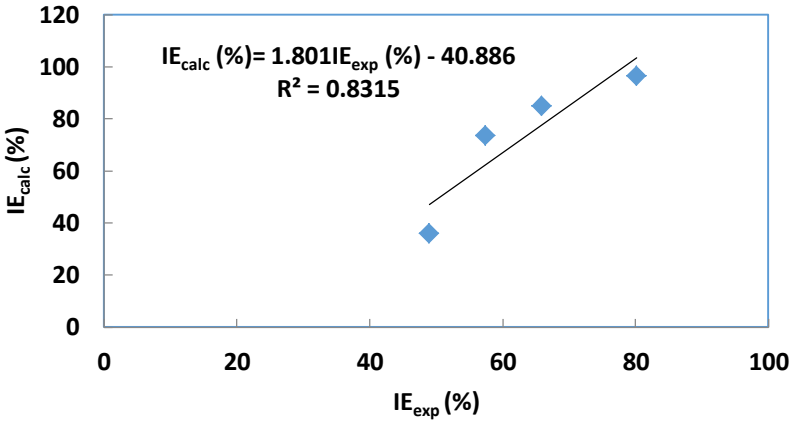

Figure 13C. Correlation between calculated and experimental inhibition efficiencies for (E_{LUMO}, E_{HOMO}, μ)

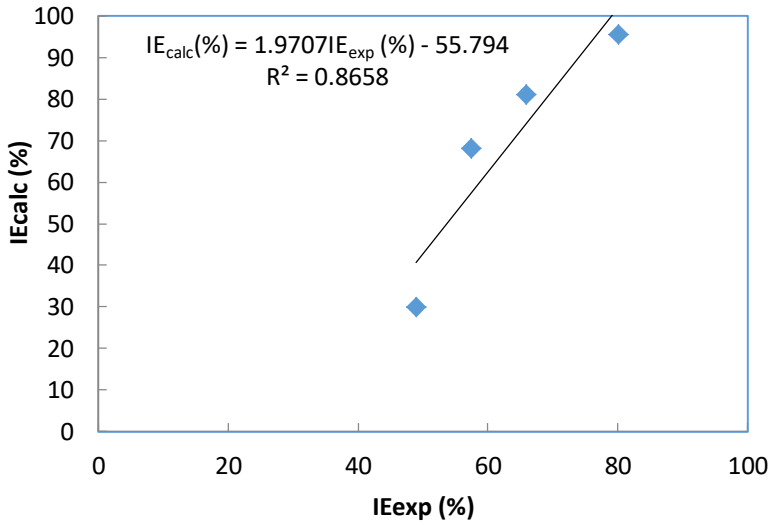

Figure 13D. Correlation between calculated and experimental inhibition efficiencies for (E_{LUMO}, ΔE, η)

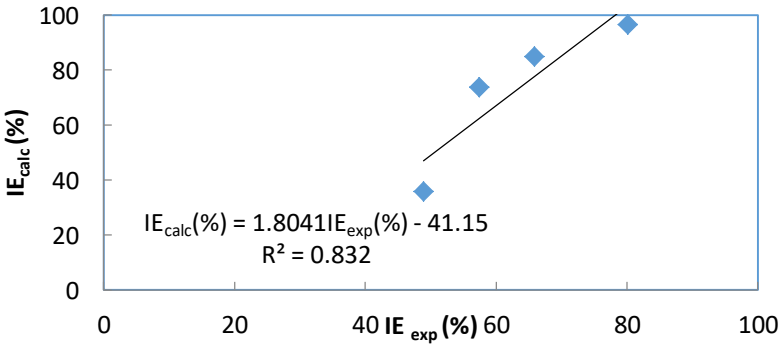

Figure 13E. Correlation between calculated and experimental inhibition efficiencies for (E_{HOMO}, ΔE, μ)

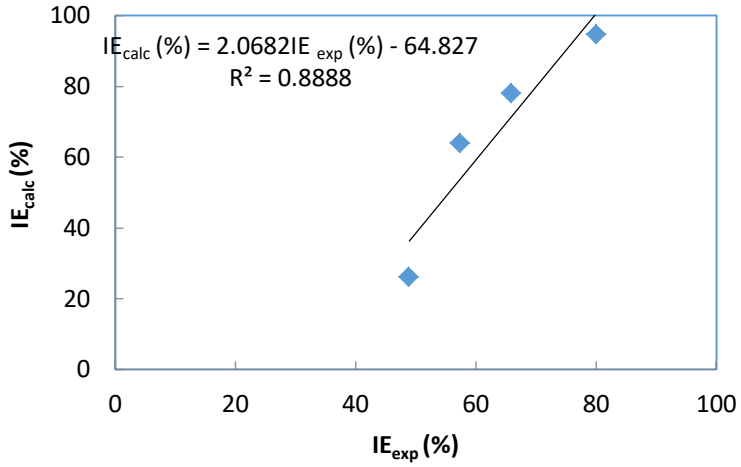

Figure 13F. Correlation between calculated and experimental inhibition efficiencies for (E_{HOMO}, ΔE ,η)

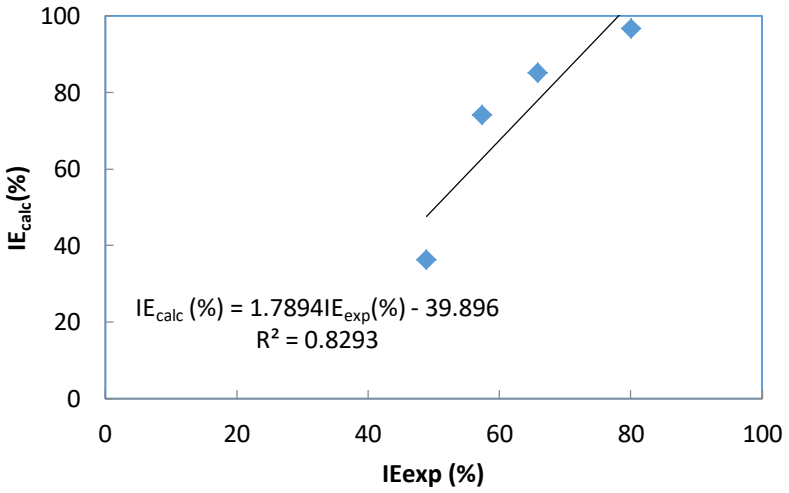

Figure 13G. Correlation between calculated and experimental inhibition efficiencies for (χ, μ η)

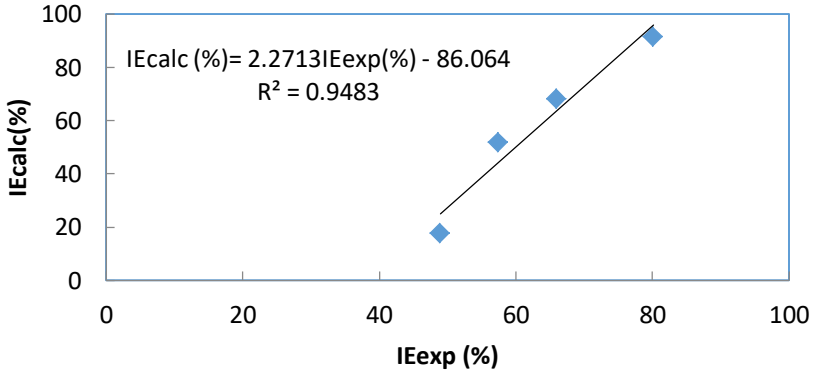

Figure 13H. Correlation between calculated and experimental inhibition efficiencies for (χ, μ, ω)

The root mean square error (RMSE):

$$RMSE = \sqrt{\sum_{i=1}^{N} \frac{|IE_{exp} - IE_{calc}|}{N}} \quad (29)$$

The mean percent deviation (MPD)

$$MPD = \frac{1}{N}\sum_{i=1}^{N} \left|\frac{IE_{exp} - IE_{calc}}{IE_{exp}}\right| \quad (30)$$

All the calculated parameters are listed in Table 8.

Table 8. Statistical parameters of the sets

Set of Parameters	R^2	SSE	RMSE	MPD
(E_{LUMO}, ΔE, μ)	0.8274	1083.25	4.033	0.261
(E_{LUMO}, ΔE, ω)	0.8105	1196.73	4.077	0.263
(E_{LUMO}, E_{HOMO}, μ)	0.8315	1062.30	4.020	0.260
(E_{LUMO}, ΔE ,η)	0.8658	938.98	3.875	0.248
(E_{HOMO}, ΔE ,μ)	0.8320	1059.99	4.019	0.260
(E_{HOMO}, ΔE ,η)	0.8880	916.85	3.736	0.236
(χ, μ η)	0.8293	1013.27	4.027	0.261
(χ, μ ,ω)	0.9483	1144.68	3.557	0.229

Referring to R^2 (0.9483), RMSE (3.557) and MPD (0.229), it is clear that the best set of parameters is (χ, μ, ω).

CONCLUSION

The results show that Theobromine is a good inhibitor for the corrosion of aluminium in 1 M HCl at the studied temperatures. The inhibition efficiencies, increase with increasing concentration of TB and decreasing temperature. The thermodynamic parameters obtained support both physical and chemical adsorption, but physical adsorption is predominant. The molecule adsorbs on aluminium according to Villamil (modified Langmuir) isotherm. The thermodynamic adsorption functions show that the adsorption is a spontaneous and exothermic process; the thermodynamic activation functions indicate an exothermic dissolution process. The presence of iodide ions affects positively the inhibition efficiency in a range of temperatures. From the dual descriptor, it is found that C (2) is the nucleophilic attack centre, whereas C (5) is the electrophilic attack centre. The sets of quantum descriptors studied show that there are good correlations (R^2>0.8) between the inhibition efficiency and the molecular descriptors. The set of three (χ, μ, ω) was found to be the best on the basis of R^2, RMSE and MDP values.

REFERENCES

1. L Guo; W Dong; S Zhang. *RSC Advances*. **2014**, 4: 41956.
2. G Sigirck; D Yildirim; T Tüken. *Corrosion Science*. **2017**, 120: 184.
3. FET Heakal; AE Elkoly. *Journal of Molecular liquids*. **2017**, 230: 395.
4. A Popova; M Christov; A Zwetanova. *Corrosion Science*. **2007**, 49: 2131.
5. Ü Ergun; KC Emregül. *Journal of Materials Engineering and Performance*. **2014**, 23: 213.
6. KF Khaled. *Corrosion Science*. **2010**, 52: 2905.
7. K Maayta; NAF Al-Rawashdeh. *Corrosion Science*. **2004**, 46: 1129.
8. M Abdallah. *Corrosion Science*. **2004**, 46: 1981.
9. B Obot; NO Obi-Egbedi; SA Umoren. *Corrosion Science*. 2**009**, 51: 1868.
10. VDPA Bhat. *Transactions of the Indian Institute of Metals*. **2011**, 64: 377.

11. C Jeyaprabha; S Sathiyanarayanan; S Muralidharan; G Venkatachari. *J Braz Chem Soc*. **2006**, 17: 61.
12. X Li; S Deng; H Fu; G Mu. *Corrosion Science*. **2008**, 50: 3599.
13. MN Arshad; A Bibi; T Mahmood; AM Asiri; K Ayub. *Molecules*. **2015**, 20: 5851.
14. CG Zhan; JA Nichols; DA Dixon. *The journal of Physical Chemistry A*. **2003**, 107: 4184.
15. A Singh; KR Ansari; A Kumar; W Liu; C Songsong; Y Lin. *Journal of alloys and compounds*. **2017**, 712: 121.
16. IA Adejoro; FK Ojo; OF Akinyele. *International Research Journal of Pure & Applied Chemistry*. **2016**, 12: 1.
17. MJ Frisch; GW Trucks; HB Schlegel; GE Scuseria; MA Robb; JR Cheeseman; G Scalmani; V Barone; B Mennucci; GA Petersson; H Nakatsuji; M Caricato; X Li; HP Hratchian; AF Izmaylov; J Bloino; G Zheng; JL Sonnenberg; M Hada; M Ehara; K Toyota; R Fukuda; J Hasegawa; M Ishida; T Nakajima; Y Honda; O Kitao; H Nakai; T Vreven; JA Montgomery; Jr., JE Peralta; F Ogliaro; M Bearpark; JJ Heyd; E Brothers; KN Kudin; VN Staroverov; R Kobayashi; J Normand; K Raghavachari; A Rendell; JC Burant; SS Iyengar; J Tomasi; M Cossi; N Rega; JM Millam; M Klene; JE Knox; JB Cross; V Bakken; C Adamo; J Jaramillo; R Gomperts; RE Stratmann; O Yazyev; AJ Austin; R Cammi; C Pomelli; JW Ochterski; RL Martin; K Morokuma; VG Zakrzewski; GA Voth; P Salvador JJ Dannenberg; S Dapprich; AD Daniels; Ö Farkas; JB Foresman; JV Ortiz; J Cioslowski; DJ Fox. *Gaussian 09 (Gaussian, Inc., Wallingford CT)*. **2009**.
18. D Becke. *The Journal of Chemical Physics*. **1986**, 84: 4524.
19. C Lee; W Yang; RG Parr. *Physical Review B*. **1988**, 37: 785.
20. NO Obi-Egbedi; IB Obot. *Corrosion Science*. **2011**, 53: 263.
21. NO Eddy; H Momoh-Yahaya; EE Oguzie. *J Adv Res*. **2015**, 6: 203.
22. G Moretti; G Quartarone; A Tassan; A Zingales. *Werkst Korros*. **1994**, 45: 641.
23. RFV Villamil; P Corio; JC Rubim; SML Agostinho. *J Electroanal Chem*. **1999**, 472: 112.
24. EE Oguzie; YLi; FH Wang. *J Colloid Interface Sci*. **2007**, 310: 90.
25. SO Adejo; MM Ekwenchi. *IOSR J Appl Chem*. **2014**, 6: 66.
26. EA Noor. *Journal of Appl Electrochem*. **2009**, 39: 1465.
27. SA Umoren; EE Ebenso. *Mater Chem Phys*. **2007**, 106: 387.
28. S Fouda; A Abd-El-Aal; AB Khandil. *Desalination*. **2006**, 201: 216.
29. N M Guan; L Xueming; L Fei. *Mater Chem Phys*. **2004**, 86: 59.
30. NO Obi-Egbedi; IB Obot. *Corrosion Science*. **2011**, 53: 263.
31. SA Umoren; EE Ebenso. *Mater Chem Phys*. **2007**, 106: 387.
32. S Xia; M Qiu; L Yu; F Liu; H Zhao. *Corrosion Science*. **2008**, 50: 2021.
33. T Arslan; F Kandemirli; EE Ebenso; I love; H Alemu. *Corrosion Science*. **2009**, 51: 35.
34. EE Ebenso; DA Isabirye; NO Eddy. *Int J Mol Sci*. **2010**, 11: 2473.
35. NO Obi-Egbedi; IB Obot. *J Mol Struct*. **2011**, 1002: 86.
36. CG Zhan; JA Nichols; DA Dixon. *The Journal of Physical Chemistry A*. **2003**, 107: 4184.
37. A Singh; KR Ansari; A Kumar; W Liu; C Songsong; Y Liu. *Journal of Alloys and Compounds*. **2017**, 712:

121.

38. G Gece. *Corrosion Science*. **2008**, 50(11): 2981.
39. H Tian; W Li; K Cao; B Hou. *Corrosion Science*. 2**013**, 73: 281.
40. S Deng; X Li; X Xie. *Corrosion Science*. **2014**, 80: 276.
41. RG Pearson. *Proceedings of National Academy of Sciences*. **1986**, 83: 8440.
42. RG Parr; RG Pearson. *Journal of American Chemical Society*. **1983**, 105: 7512.
43. RG Parr; SR Gadre; LJ Bartolotti. *Proceedings of National Academy of Sciences of the United States of America*. **1979**, 76: 2522.
44. J Haque; KR Ansari; V Srivastava; MA Quraishi; IB Obot. *Journal of Industrial and Engineering Chemistry*. **2017**, 49: 176.
45. RG Pearson. *Inorganic Chemistry*. **1988**, 27: 734.
46. N Kovacevic; A Kokalj. *Journal of Physical Chemistry C*. **2011**, 115: 24189.
47. RG Pearson. *Coordination Chemistry Reviews*. **1990**, 100: 403.
48. A Kokalj; N Kovacevic. *Chemical Physics Letters*. **2011**, 507: 181.
49. RG Parr; L Svenpaly; S Liu. *Journal of the American Chemical Society*. **1999**, 121: 1922.
50. P Geerlings; F De Proft; W Langenaeker. *Chemical Reviews*. **2003**, 103: 1793.
51. A Kokalj. *Electrochimica Acta*. **2010**, 56: 745-755.
52. J Olah; CV Alsenoy. *The Journal of Physical Chemistry A*. **2002**, 106: 3885.
53. C Morell; A Grand; A Toro Labbé. *J Phys Chem* A. **2005**, 109: 205.
54. C Morell, A Grand; A Toro Labbé. *Chem Phys Lett.* **2006**, 425: 342.
55. JI Martinez-Araya. *Journal of Mathematical Chemistry*. **2014**, 53: 451.
56. J Fang; J Li. *Journal Mol Structure (THEOCHEM)*. **2002**, 593: 179.
57. B Obot; NO Obi-Egbedi; SA Umoren. *Corrosion Science*. **2009**, 51: 276.
58. R Leach. *Prentice Hall*. **2001**.
59. I Lukovits; A Shaban; E Kalman. *Russ J Electrochem*. **2003**, 39: 177.